ISSN 0016-8521, Geotectonics, 2012, Vol. 46, No. 3, pp. 171–184. © Pleiades Publishing, Inc., 2012.
Original Russian Text © S.Yu. Sokolov, V.G. Trifonov, 2012, published in Geotektonika, 2012, Vol. 46, No. 3, pp. 3–18.

Role of the Asthenosphere in Transfer and Deformation of the Lithosphere: The Ethiopian–Afar Superplume and the Alpine–Himalayan Belt

S. Yu. Sokolov and V. G. Trifonov

Geological Institute, Russian Academy of Sciences, Pyzhevskii per. 7, Moscow, 119017 Russia
e-mail: sysokolov@yandex.ru

Received September 27, 2011

Abstract—Seismic tomographic data showing the mantle structure of the Ethiopian–Afar superplume and various segments of the Alpine–Himalayan Orogenic Belt and their relationships with the adjacent megastructures of the Earth are presented. These data and their correlation with the geological evidence lead to the conclusion that lateral flows of mantle material are crucial for the evolution of the Tethys and its closure in the Cenozoic with transformation into an orogenic belt. The lateral flow of hot upper mantle asthenospheric matter spreading from the stationary superplume extending in the meridional direction (in present-day coordinates) was responsible for the accretion of the fragments torn away from Gondwana to Eurasia and for the development of subduction at the northeastern flank of the Tethys. The characteristic upper mantle structure of cold slabs passing into nearly horizontal lenses with elevated seismic wave velocity in the lowermost upper mantle is currently retained in the Indonesian segment of the orogenic belt. In the northwestern segments of this belt, a hot asthenospheric flow reached its northern margin after closure of the Tethys and onset of collision, having reworked the former structure of the upper mantle and enriched it in aqueous fluids. The effect of this active asthenosphere on the lithosphere gave rise to intense Late Cenozoic deformation, magmatism, and eventually resulted in mountain building.

DOI: 10.1134/S0016852112030053

INTRODUCTION

According to the classic plate-tectonic concept, the lithospheric plates embracing the Earth's crust and the uppermost mantle down to a depth of 50–200 km move from a spreading zone toward subduction and collision zones along the paths marked by transform fracture zones. The mechanisms of this movement are a matter of debate. Push-apart of plates by magmatic material injected into spreading zones is proposed as one possible mechanism; however, the ratio of the dimensions characterizing vertical flow of hot material beneath the mid-ocean ridges and the plates pushed away is ~1/40 (seismic tomographic data), and this makes this mechanism unlikely without the involvement of additional effects [32]. A similar reasoning compels us to rule out a slab pull effect of subducted slabs, although a dragging effect is undoubtedly important for plunging of slabs because of their higher density relative to the hot mantle and weighting as a result of phase transformation [33].

Therefore, the idea arose that the plates move by flows of underlying mantle, primarily, of the asthenosphere. The hypotheses of the self-dependent movement of plates over a viscous asthenoapheric layer under the effect of inertial and rotational mechanisms are out of the scope of this paper. Some authors consider the asthenosphere as merely a product of phase transformation related to variations of temperature (T) and pressure (P) with depth. According to this viewpoint, the asthenosphere appears in the upper mantle at a depth of ~100 km beneath all continents and is not tectonically predetermined [59]. Most researchers, assuming P–T preconditions of the asthenophere, emphasize its heterogeneity and the variation in depth of its upper edge correlated with its localization beneath different domains of the continental lithosphere [16, 42, 54]. In the opinion of Letnikov [16], the links between lithospheric plates and the asthenosphere is proved by the inverse correlation between the thickness of the granite-gneiss layer and the depleted lithospheric mantle, on the one hand, and the depth and thickness of the asthenosphere, on the other hand. This viewpoint assumes not only the joint movement of the asthenosphere and lithosphere but also the geodynamic impact of the former on the latter. Asthenospheric flows are regarded as elements of whole-mantle convection [23, 24, 38], convection cells in the upper mantle [22], or as a result of interference of both convection levels [5, 11].

The idea of mantle convection as a mechanism of lithospheric plate motion is tested by the data of seismic tomography. It has been established that in the subduction zone at the western Pacific margin, some subducted slabs with a high Q-factor are traced as seis-

mofocal zones to a depth of 650 km [39] and as high-velocity bodies to 900–1000 km below the upper mantle [47]. This seemingly points to whole-mantle convection. More detailed seismic tomography of the Aleutian, Kurile–Kamchatka, and Japanese island arcs [7, 49] has shown, however, that only in 5 of 22 transverse sections do slabs extend below 670 km. In other sections, slabs pass into a lenticular layer at a depth of 410 to 670 km. In the cases when slabs go deeper, this lenticular layer is also detected in the section and expresses a sharper distribution of V_p velocities than the downward continuation of the slab. Zhao, Piraino, and Liu [7] termed this layer a large mantle wedge (LMW). As a rule, a lenticular layer of lowered V_p velocities is detected above the LMW.

At the same time, since the early publications on seismic tomography, it has been shown that the low-velocity columns, which could be interpreted as ascending mantle flows, do not extend deeply in the mantle, whereas flows ascending from the lower mantle are located elsewhere [1]. Initially, two such deep-seated superplumes—the Central Pacific and Ethiopian–Afar—were recognized. Later on, similar though weaker ascending flows were detected beneath Iceland, the Cape Verde Islands, the Canaries, and some other volcanic provinces. When these flows approach a mid-ocean ridge from below, the products of volcanic activity related to the ridge are mixtures of MORB and deep enriched varieties of basalts. Some such flows, e.g., the Central Pacific, do not ascend above the asthenosphere or are separated from it by high-velocity bodies at a depth of ~670 km (Cape Verde Islands). In addition to superplumes ascending from the lower mantle and traceable from almost the core–mantle boundary, more numerous plumes (manifestations of upwelling) ascend from the transitional layer (410–670 km), e.g., the plume beneath the Baikal Rift System [7], or often from even higher levels in the mantle [11].

Anomalies of seismic wave velocities (deviations from average statistical values characteristic of certain depths) corresponding to ascending hot and descending cold mantle flows reach only a few percent in the asthenosphere and local segments of subducted slabs. Elsewhere in the mantle, they are lower, deviations of 0.25% for V_p and 0.5% for V_s, i.e., 0.02–0.06 km/s, deemed to be significant. At the same time, V_p in the mantle increases with depth from ~8 to ~13 km/s and V_s from 4.3 to 7.0 km/s. At certain levels, the velocities change by significant values of km/s. Such jumps are referred to variations in rock density, which cannot be caused only by compaction or decompaction of rocks under the load of overlying rocks but suggest a change in the crystal chemistry of minerals.

These transformations, confirmed by laboratory experiments at superhigh pressure and temperature, have been described in the literature and recently summarized in [28]. These publications rid us from the necessity of detailed discussion in this paper. Note only that at a depth of 50–100 km pyroxenes of mafic and ultramafic rocks are transformed into garnets with a higher density. Several other seismic discontinuities are detected below in the upper mantle. The most distinct and extensive boundaries occur at depths of ~410 and 670 km. The former marks the transition of orthorhombic olivine to the variety with spinel structure (wadsleyite transformed at a depth of ~520 km into ringwoodite), the density of which increases by 8%. Clinopyroxene is transformed into wadsleyite and stishovite at approximately the same depth. Within a depth interval of 410 to 500 km, pyroxenes acquire a more compact ilmenite-type structure. Thus, garnet, spinel, and silicates with ilmenite structure dominate at a depth of 410–670 km. At a greater depth, these minerals are replaced by denser perovskite-like phases occupying ~80% of the volume of the middle[1] and lower mantle [28].

The aforesaid shows that the jumps at seismic discontinuities and partly the general increase in the seismic wave velocity with depth are caused by modification of the crystal chemistry of mantle minerals, while the bulk chemical composition remains rather uniform. The variation in velocity probably reflects variation in the mantle density with depth. The descending and ascending flows of the mantle material are traced through the aforementioned seismic boundaries, and this implies that the flows undergo the same change in crystal chemistry as the surrounding mantle, retaining a difference in temperature. Because of the temperature difference, the transition of olivine into a spinel phase, as well as of pyroxene with segregation of stishovite, proceeds in a cold slab at a lower pressure at a depth of 300–380 km. In hot superplumes, the depth of transition probably increases. It should also be kept in mind that phase transitions may be exothermic, e.g., transformation of olivine into spinel or pyroxene into the phase with ilmenite structure, or endothermic, for example, transition to perovskite-type structure [33], with additional complication of the seismic tomography patterns.

The water content in the asthenosphere is a principal parameter determining its geodynamic role. Ringwood [29] estimated the water content at 0.1%. According to the data published by Pugin and Khitarov [26], the water content in the mantle is measured by 0.1%. At the same time, Letnikov [17, 19, 20] supposes that deep fluids play an important role in the formation of lithospheric (including crustal) magma sources and in metamorphism of the lithosphere. He suggests that the asthenosphere is the main source of fluids and also assumes that they may be supplied from a greater depth [18, 21].

No direct evidence for the occurrence of water in the sublithospheric mantle is available because the

[1] According to [27], the middle mantle occupies a depth interval of 900–1700 m.

deep H_2O-bearing xenoliths and exhumed rocks could have been metamorphosed at a shallow depth with loss of water. According to petrologic and geochemical data, most minerals in the sublitospheric mantle are anhydrous [30]. Only the rocks within the depth interval 410–670 km may be an exception. The crystal chemical structure of wadsleyite and ringwoodite allows replacement of a part of the oxygen anions in anhydrous minerals with a hydroxyl group [50, 57]. The subducted slabs, which contain incompletely dehydrated amphibolites and metasedimentary rocks, can be a source of hydroxyl. As was said above, such slabs are transformed into almost horizontal high-velocity lenses at a depth of 410–670 km [24]. The appreciable attenuation of shear waves along with insignificant change of their velocities [52] and increased electric conductivity [51] indicate that fluids occur at those depths.

As concerns deeper sources of aqueous fluids, recent data on the density of the Earth's core allows the occurrence of hydrogen therein. Iron hydride is stable at the temperature and pressure characteristic of the lower mantle [28], but the minerals of the middle and lower mantle contain a minimal amount of oxygen, and this rules out its coupling with hydrogen. Such an opportunity appears only at the depth interval 410–670 km. Therefore, it is assumed that potential sources of water fluid occur in a mantle superplume above a depth of 670 km, and particularly in plumes ascending from the transitional layer or asthenosphere.

Thus, the manifestations of whole-mantle convection are substantially distorted and supplemented by displacements of rock masses in the upper mantle above a depth of ~670 km. These displacements and the probable occurrence of aqueous fluids allow us to pose a question on the important tectonic role of the upper-mantle processes. The aim of the proposed paper is to present and discuss seismic tomographic evidence for upper mantle movements with allowance for mineral transformations and to set forth their possible impacts on the movement and deformation of the lithospheric plates. The Ethiopian–Afar superplume and the Alpine–Himalayan Orogenic Belt are subjects of this study. Data on other regions are referred to for comparative purposes.

THE ETHIOPIAN–AFAR SUPERPLUME AND THE ALPINE–HIMALAYAN OROGENIC BELT: SEISMIC TOMOGRAPHIC DATA

Consideration of the seismic tomographic data on northeastern Asia [7] has shown that the processed data from the global network of stations, though worse in resolution compared to the data of the regional seismological network, nevertheless give a generally similar pattern. Therefore, the seismic tomographic data obtained on the basis of the global network were used for the study of the Ethiopian–Afar superplume and the Alpine–Himalayan Belt [44, 48, 61]. When these data are interpreted, their lower spatial resolution in comparison with the regional models should be kept in mind. In particular, this resolution does not allow discrimination of the lithosphere and asthenosphere. Other geophysical evidence is needed for this purpose. For example, the lower average seismic wave velocities beneath continents at a depth down to 100 km are interpreted as evidence for emergence of the asthenosphere.

The lines of the seismic tomographic sections are shown in maps of V_p and V_s variations in the surface layer 100 km in thickness (Figs. 1, 2). The sections themselves (Figs. 3–6) are based on these data [44, 48, 61]. The anomalous V_p and V_s values are expressed in percent as deviations from the average value for the given layer. The $dV_p = 0.25–0.8\%$ and $dV_s = 0.5–2.0\%$ are accepted as super noise level and $dV_p > 0.8\%$ and $dV_s > 2\%$ as much higher than noise. Systems of mid-ocean ridges are distinctly seen in the V_s field with two exceptions—the Knipovich Ridge and a segment of the African–Antarctic Ridge near the Kerguelen Plateau—and are not expressed almost at all in the V_p field. In contrast, the collision zones of the Earth, in particular, the Alpine–Himalayan Belt, are clearly seen in the V_p field.

Sections 1–1' across the Tonga–Kermadec arc show that the zone of increased and highly increased dV_s corresponding to the seismic focal zone passes at a depth of 400–800 km into the horizontal high-velocity lens beneath the subcontinental Tonga Plain (Fig. 3) similar to those revealed at the northeastern active margin of Asia [7]. A similar passage is revealed beneath the Andaman–Indonesian arc (Fig. 3, sections 2–2') and is outlined at a depth of 400–500 km beneath the Cretan–Hellenic arc (Fig. 3, sections 6–6').

Another situation is characteristic of the Tibetan–Himalayan segment of the belt (Fig. 4, section 3–3'). The layer of highly increased dV_s down to the depth of 100–300 km extends here from the Himalayas to the northern margin of the Tien Shan and continues as a high-velocity layer beneath the Indian Platform and the Kazakhstan–West Siberian segment of the Eurasian Plate. The high-velocity layer thickens to 400 km beneath Southern Tibet near the Neothetian Suture (Indus–Zangpo Zone). One more nearly horizontal high-velocity lens is detected at a depth of 600–700 km. It cannot be ruled out that a part of the upper high-velocity layer and this lens are transformed relics of the Neotethian slab flattened at a depth. In the dV_p section, a similar high-velocity lens is traced from the southern margin of the Indian Platform to the northern margin of Tibet at a depth of 100–300 km. The greatest thickness of this layer and the highest dV_p values are established beneath Southern Tibet. To the north, the averaged dV_p values in the upper mantle decline to a moderate level and one more high-velocity lens appears in the south of Western Siberia. A domain of lower dV_p occurs below the high-velocity

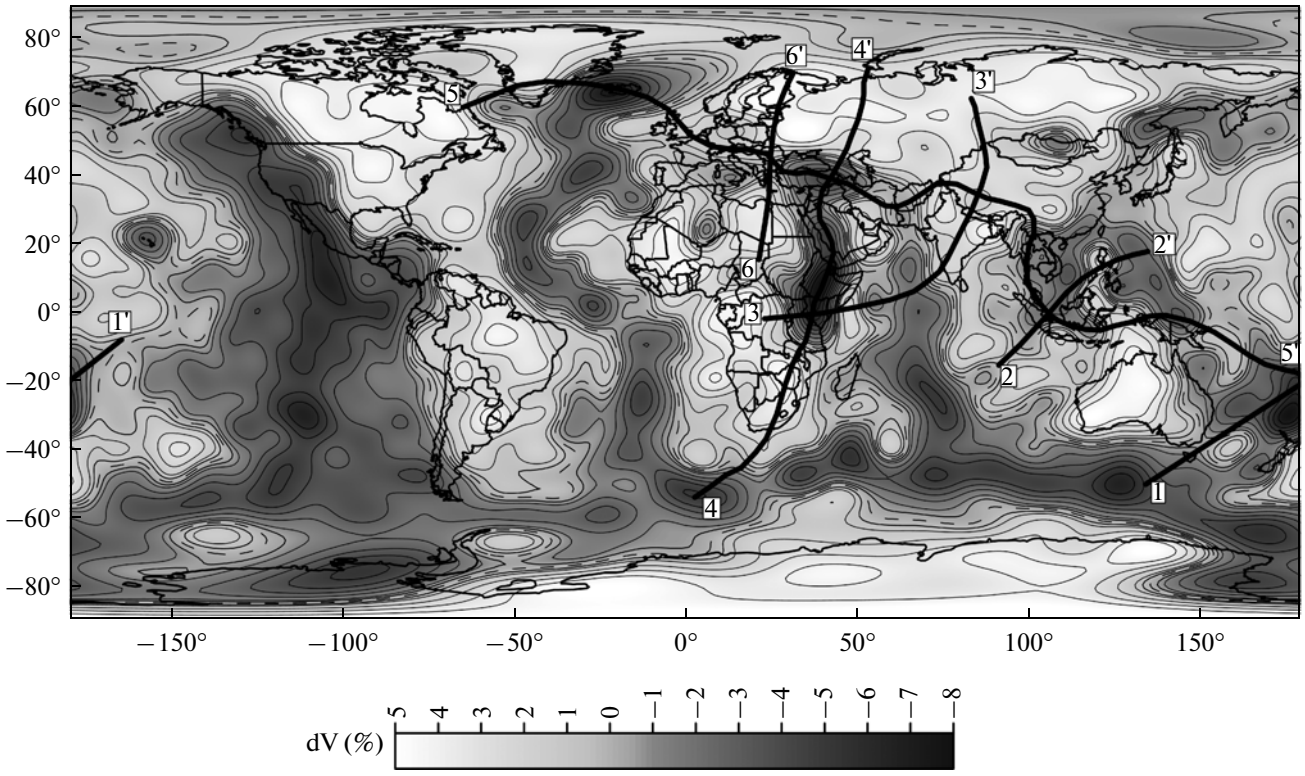

Fig. 1. Global distribution of dV_s at a depth up to 100 km. Compiled by S.Yu. Sokolov after the data published in [43, 47, 60]. Lines of sections (Figs. 3–6) are shown. Contour lines are spaced at 1% for S-waves; the dashed line corresponds to zero value.

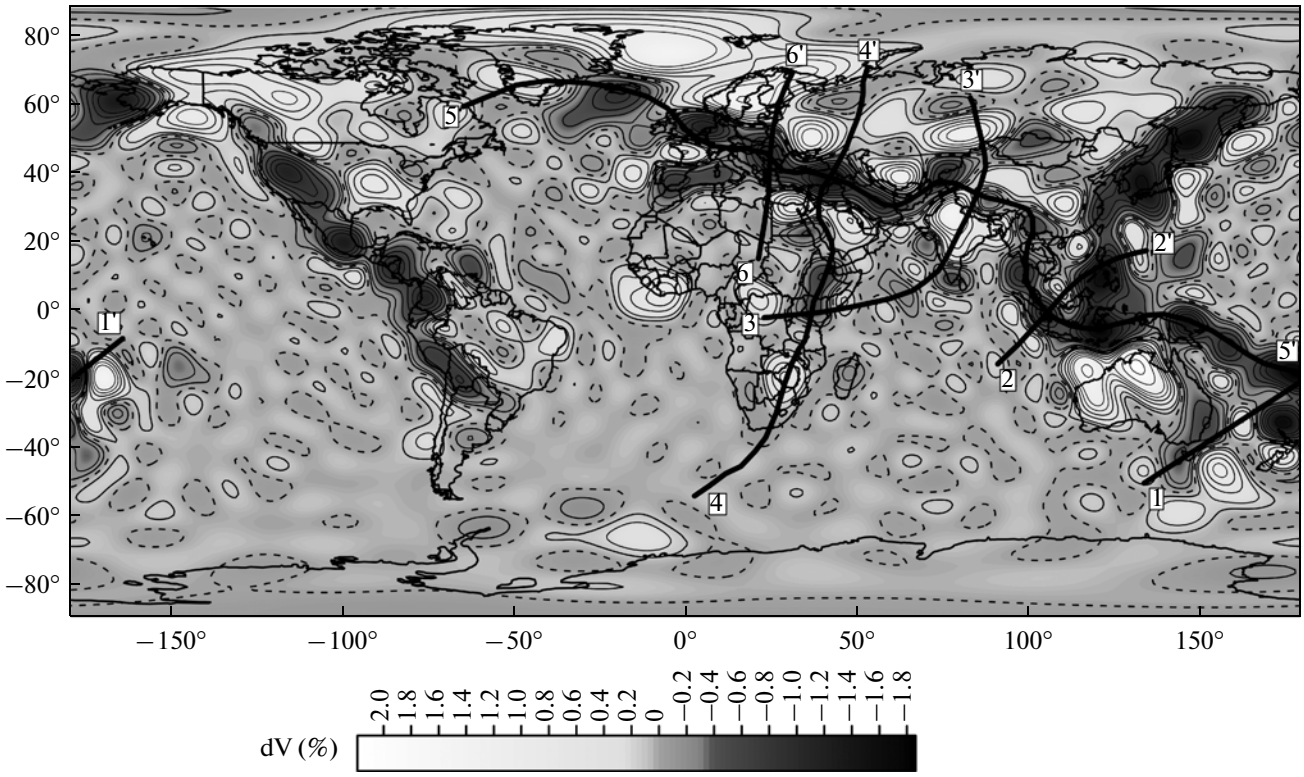

Fig. 2. Global distribution of dV_p at the depth up to 100 km. Compiled by S.Yu. Sokolov after the data published in [43, 47, 60]. Lines of sections (Figs. 3–6) are shown. Contour lines are spaced at 0.2% for P-waves; the dashed line corresponds to zero value.

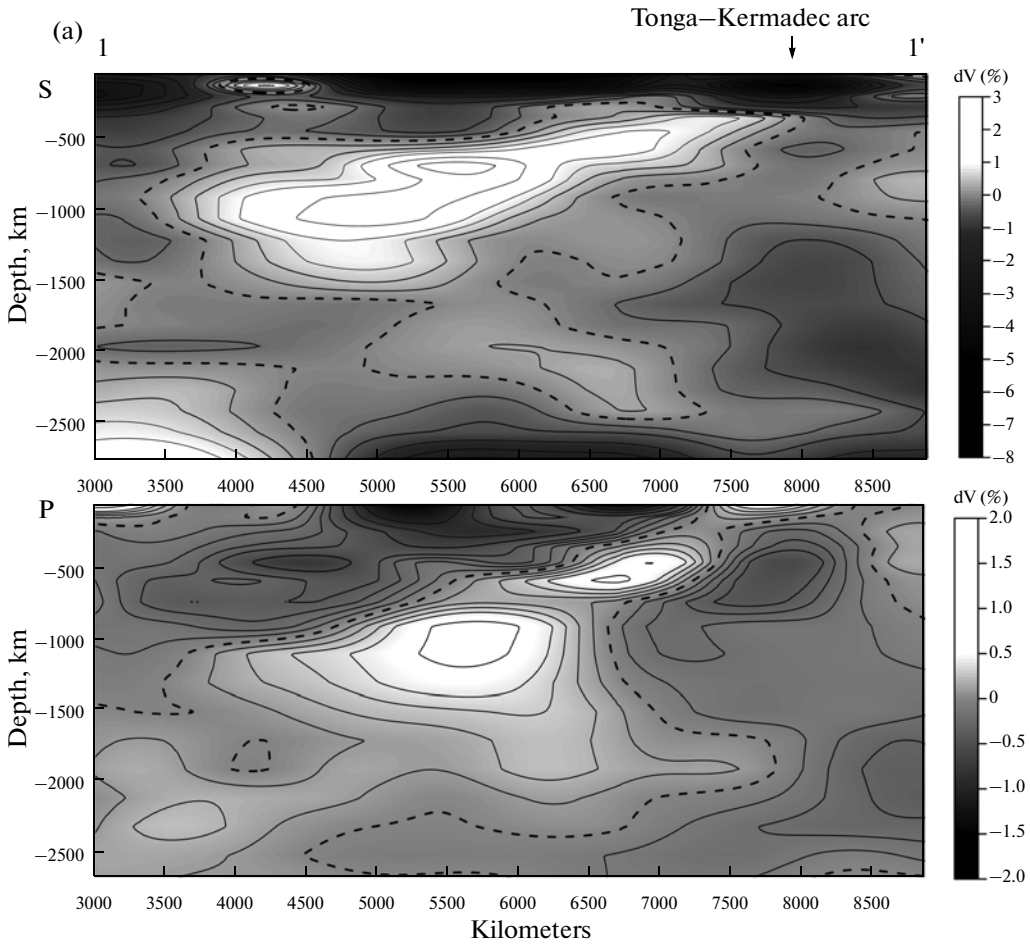

Fig. 3. Transverse seismic tomographic dV_s and dV_p sections along lines: (a) 1–1' across the Tonga–Kermadec arc; (b) 2–2' across the Andaman–Indonesian arc; (c) 6–6' across Cretan–Hellenic arc and the Carpathians. Compiled by S.Yu. Sokolov after the data published in [43, 47, 60]. Contour lines are spaced at 0.5% for S-waves and 0.25% for P-waves; the dashed line corresponds to zero value.

layer as a narrow (400–500 km) lens beneath the Indian Platform. This domain is reduced beneath Southern Tibet and swells to a depth of 300–800 km beneath High Asia from Tibet to the Tien Shan, where locally reaches very low dV_p values. In the lower mantle, a poorly delineated and fragmented zone of slightly lowered dV_p values tilted to the southwest occurs beneath this thickened lens. In the dV_s section, the above-mentioned features are less distinct. A domain of slightly lowered dV_s values is situated beneath High Asia, and the tilted zone in the lower mantle is noted by moderate dV_s against the background of slightly elevated values beneath the adjacent territories.

Of principal importance are the seismic tomographic sections across the Ethiopian–Afar superplume and the Arabian–Iranian segment of the Alpine–Himalayan Belt (Fig. 5, sections 4–4'). Relatively thin upper mantle lenses with very low dV_s values are seen in the section no deeper than 200 km. These are a short lens near Bouvet Island and a long lens, which extends beneath the East African Rift System and the Red Sea Rift to southern Arabia. The northern lens extends northward to the Greater Caucasus, where it is characterized by lower dV_s values. A wide domain of lowered and slightly lowered dV_s values is traced below down to bottom of the mantle. The upper part of this domain corresponds to the territory from Malawi to the Red Sea, and, being tilted to the south, is located beneath South Africa at the lower-mantle level. This domain is regarded as the Ethiopian–Afar superplume. The upper mantle of the African and Eurasian plates is distinguished by increased dV_s values. A low-velocity wedge plunges from the Scythian Platform beneath the Greater Caucasus, where it flattens and is traced to the Lesser Caucasus, gradually losing its specificity. In the dV_p section, the Ethiopian–Afar superplume is also expressed as a wide domain of increased dV_p values tilted to the south. In the upper mantle, this domain is traced to a depth of 600–800 km from Malawi to the Lesser Caucasus. Its segments beneath the Kenyan Rift, Afar, and the Armenian Highland are distinguished by highly

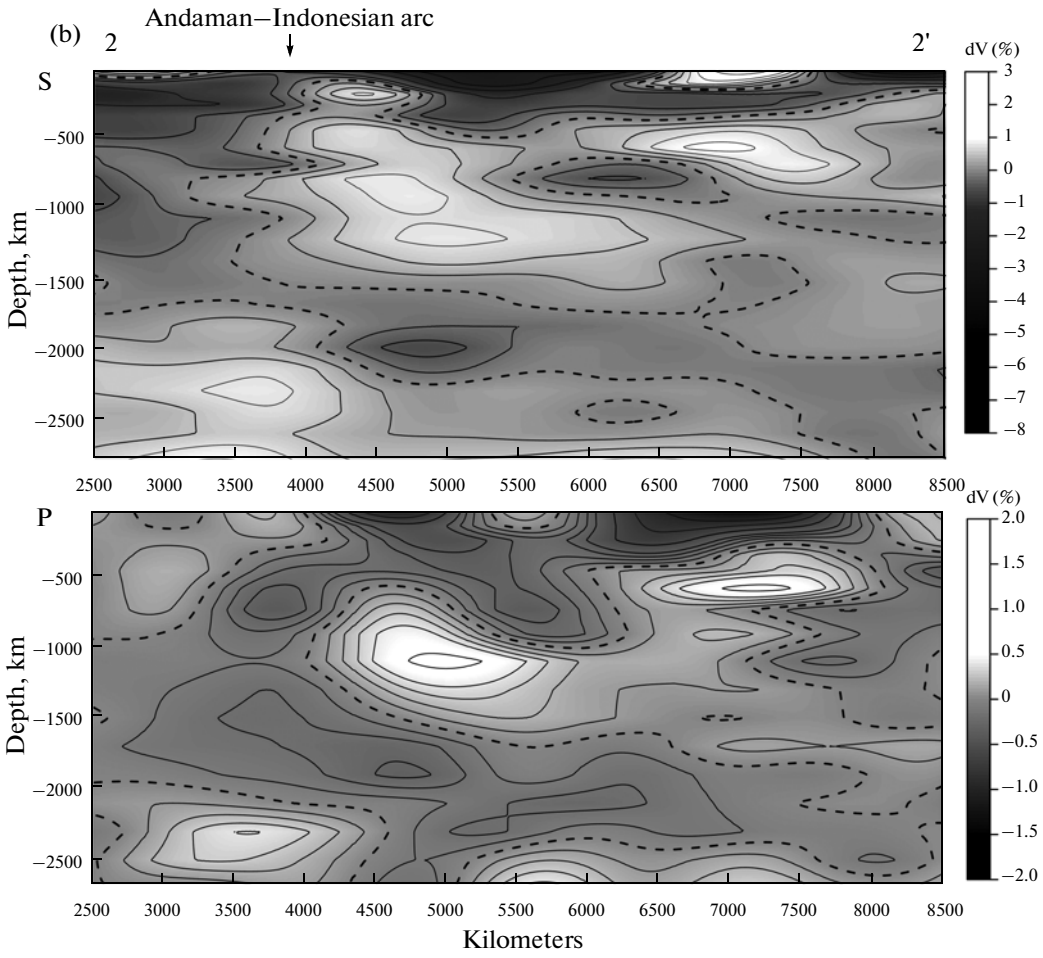

Fig. 3. (Contd.)

increased dV_p. Beneath the Greater Caucasus the thickness of this domain is abruptly reduced and limited from below by the high-velocity wedge plunging from the Scythian Platform. The upper mantle of South Africa and the East European Platform is characterized by slightly elevated and medium dV_p values.

The transverse sections are supplemented by longitudinal sections 5–5' oriented along the axis of the Alpine–Himalayan Belt and extending from the Tonga–Kermadec arc via the backarc basins of the Andaman–Indonesian arc, Tibet, the Pamir, Afghanistan, Iran, and the Lesser Caucasus to Anatolia and the Carpathians and then via the West European Hercynides to Iceland (Fig. 6). These sections are important for understanding of the deep structure of the belt for two reasons.

First, they make it possible to look at the structures delineated in the transverse sections in another perspective. For example, the longitudinal sections confirm passing of the slab beneath the Tonga–Kermadec arc in a nearly horizontal zone of elevated V_p and V_s values at a depth of 600–800 km. In the dV_s section, this zone is supplemented by nearly horizontal high-velocity lenses at depths of 100–200 and 350–500 km at the western Pacific margin and at a depth of ~200 km between the Papua New Guinea arc and the eastern flank of the Andaman–Indonesian arc. The two-stage structure of the upper mantle beneath Tibet revealed in transverse section 3–3' (elevated V_p above and lowered V_p below) is confirmed by the longitudinal section, where such a structure is detected over the entire territory from the eastern margin of Tibet to the Pamir–Hindu Kush. In the west, from Afghanistan to the Carpathians, a layer of lowered and deeply lowered dV_p values is depicted at a depth down to 200–300 km and extends beneath the West European Hercynides. The fact that the same structures are detected in both longitudinal and transverse sections indicates that the revealed variations are related to real mantle inhomogeneities rather than to the effect of anisotropic propagation of seismic waves.

Second, sections 5–5' demonstrate segmentation of the belt known from the relationships between the Late Cenozoic crustal structural elements [37]. This segmentation is expressed better in the dV_p section, where the difference of the segments is traced

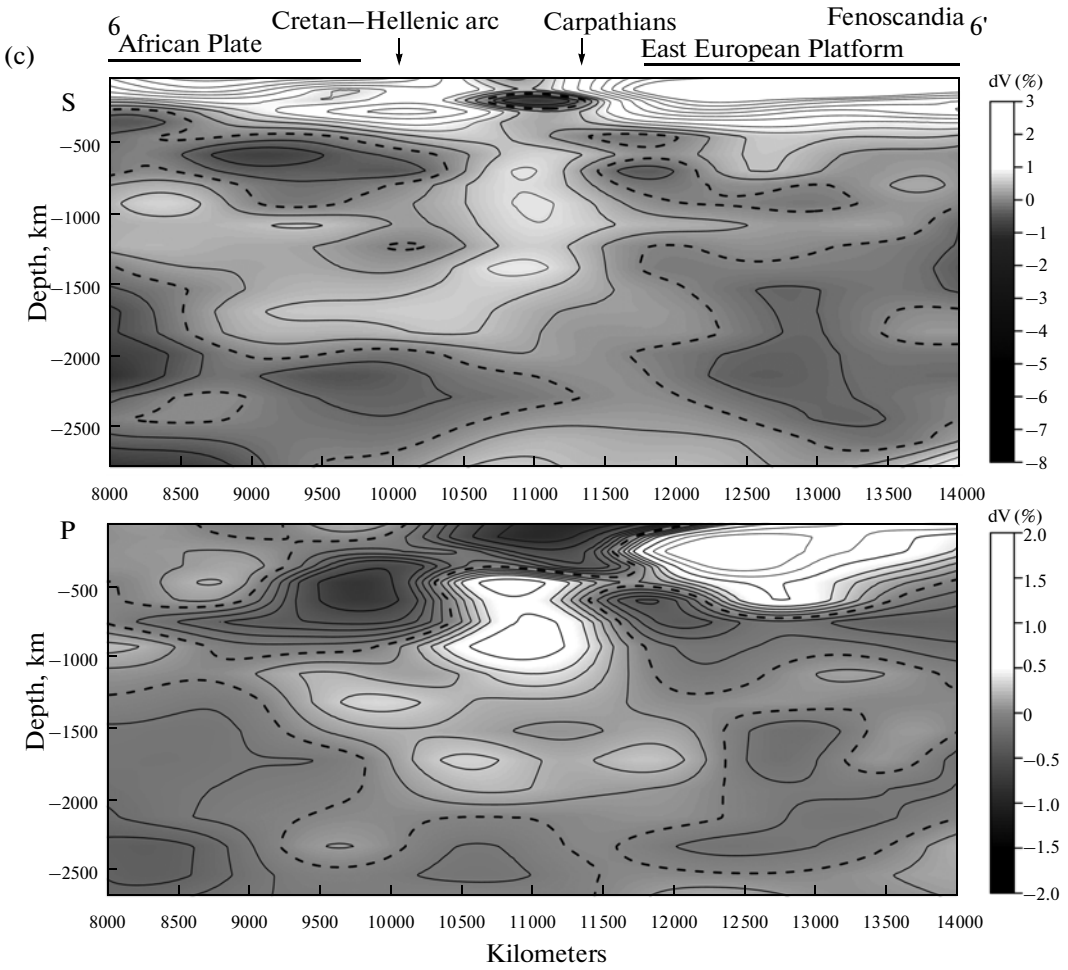

Fig. 3. (Contd.)

throughout the upper mantle. The boundary between the southeastern island-arc and the Tibetan section types approximately coincides with the fault zone of 105° E between the corresponding segments of the belt, whereas the boundary between the Tibetan and the Iran–Caucasus section types fits the Darwaz–Chaman Fault Zone between the Pamir–Himalayan and the Arabian–Iranian segments.

The Iceland upper mantle low-velocity domain, which is also seen in sections 5–5', extends into the lower mantle, where its contrast with respect to the surrounding mantle decreases. This low-velocity domain is interpreted as the Iceland superplume. Despite the noticed uncertainties, the axis of the low-velocity domain declines to the southeast down to a depth of ~1500 km.

COMPARATIVE ANALYSIS

At a depth down to 100 km, V_s lowers beneath almost all oceanic volcanic spreading zones and the adjacent regions of the World Ocean (Fig. 1). Especially low velocities are fixed in the Ethiopian–Afar and Iceland superplumes, as well as in some areas of the Central and South Pacific. Lower V_s values are also noted in the marginal seas between the Andaman–Indonesian and Mariana arcs, near the Tonga–Kermadec arc, in the Sea of Okhotsk, and in the west of the Arabian Plate and the Caucasus region. Beneath the continents, the V_s values are increased because the upper surface of the asthenosphere is depressed there.

The significant negative V_s anomalies beneath the Mid-Atlantic Ridge wane at a depth of 100–200 km and disappear at a level of 250–300 km, remaining with lower values only in the Iceland superplume [31]. A similar pattern is established in other oceanic spreading zones. At the same depths, the most voluminous Central Pacific superplume passes into the near-horizontal low-velocity zone, which merges with the East Pacific spreading zone. In contrast, the Ethiopian–Afar superplume, which also involves the region of the Kenyan Rift in the south, is traced up to the Earth's surface. In the related lateral lens of negative V_s anomalies, the lowest dV_s values are noted immediately under the lithosphere. This lens extends to the Greater Caucasus and is interpreted as a lateral

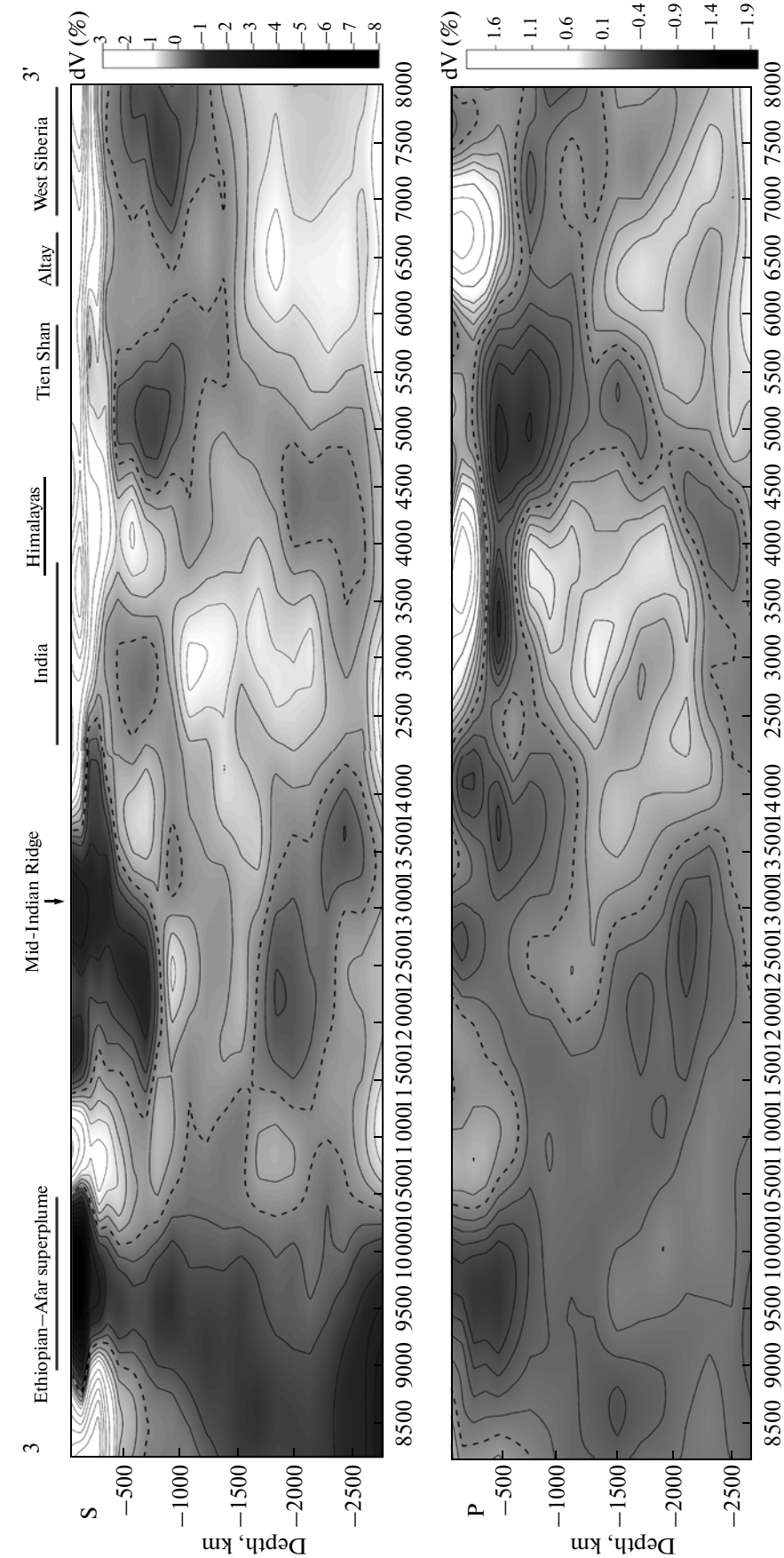

Fig. 4. Seismic tomographic dV_s and dV_p sections along line 3–3' from Kenya via the Mid-Indian Ridge, Indian Platform, and High Asia to the epi-Paleozoic West Siberian Platform. Compiled by S.Yu. Sokolov after the data published in [43, 47, 60]. Contour lines are spaced at 0.5% for S-waves and 0.25% for P-waves; the dashed line corresponds to zero value.

asthenospheric flow of superplume material, which provoked recent volcanic activity in the region [6, 40].

The age and specificity of volcanism allow us to judge about the propagation of this flow. Mantle-derived volcanic activity is documented in Ethiopia from the Eocene and in Kenya from the Oligocene [6, 40]. About 32–30 Ma ago, volcanism spread over the northeastern wall of the Red Sea Rift and continued there up to 20 Ma ago and locally later; the peak fell on 24–21 Ma ago [46, 56]. The Cenozoic volcanism in the western Arabian Plate started ~26 Ma ago in the Jebel Arab Highland (Harrat Ash Shaam) in southern Syria and adjacent Jordan; 18–16 Ma ago the volcanic front reached the northern margin of the Arabian Plate [60]. The basalts of central and northern Arabia are similar in chemistry and thus in formation conditions [58]. The volcanic districts at the western margin of the Arabian Plate are inherited and the largest of them functioned for a long time, e.g., up to 25 Ma on the Jebel Arab Highland. Even particular feeding fault zones remained active for several million years. No signs of unidirectional migration of volcanism are noted. Because the Arabian Plate substantially displaced northward during this time, the inherited volcanic activity implies that the magma sources moved together with the plate, i.e., were localized within the lithospheric mantle [60]. This geological conclusion is consistent with the results of geochemical study [53, 56].

It is suggested that in the process of movement, the asthenospheric flow from the Ethiopian–Afar superplume deformed the bottom of the lithospheric plate. Magmatic sources arose in the sites of local decompression. Under geodynamic conditions suitable for the formation and functioning of conduits, these sources manifest themselves in volcanic eruptions. Because the magma sources were maintained by sublithospheric flow, they enabled the ejection of volcanic material at the same place during a long time. The composition of that flow changed during its movement due to partial crystallization and involvement of local asthenospheric material, which also melted in magma sources. As a result, the geochemical features of the Ethiopian–Afar superplume are established in the basalts from the southern and southwestern Arabian Plate [41, 43, 45] but are not identified to the north in Syria [53].

The sublithospheric flow penetrated northward into the Arabian–Iranian segment of the Alpine-Himalayan belt only as early as the subduction of Tethian relics at the southern margin of the belt completed in the early Miocene [6, 55]. The intense volcanism, which rapidly spread from the Armenian Highland and Central Anatolia to Mount Elbrus, started in the late Miocene and continued in the Pleistocene and locally in the Holocene. A wide range of volcanic rocks from basalt to rhyolite was formed. These rocks primarily belong to the calc-alkaline series; the alkalinity of the rocks increases at the periphery of the volcanic field [9, 12, 13]. The thermodynamic calcula-

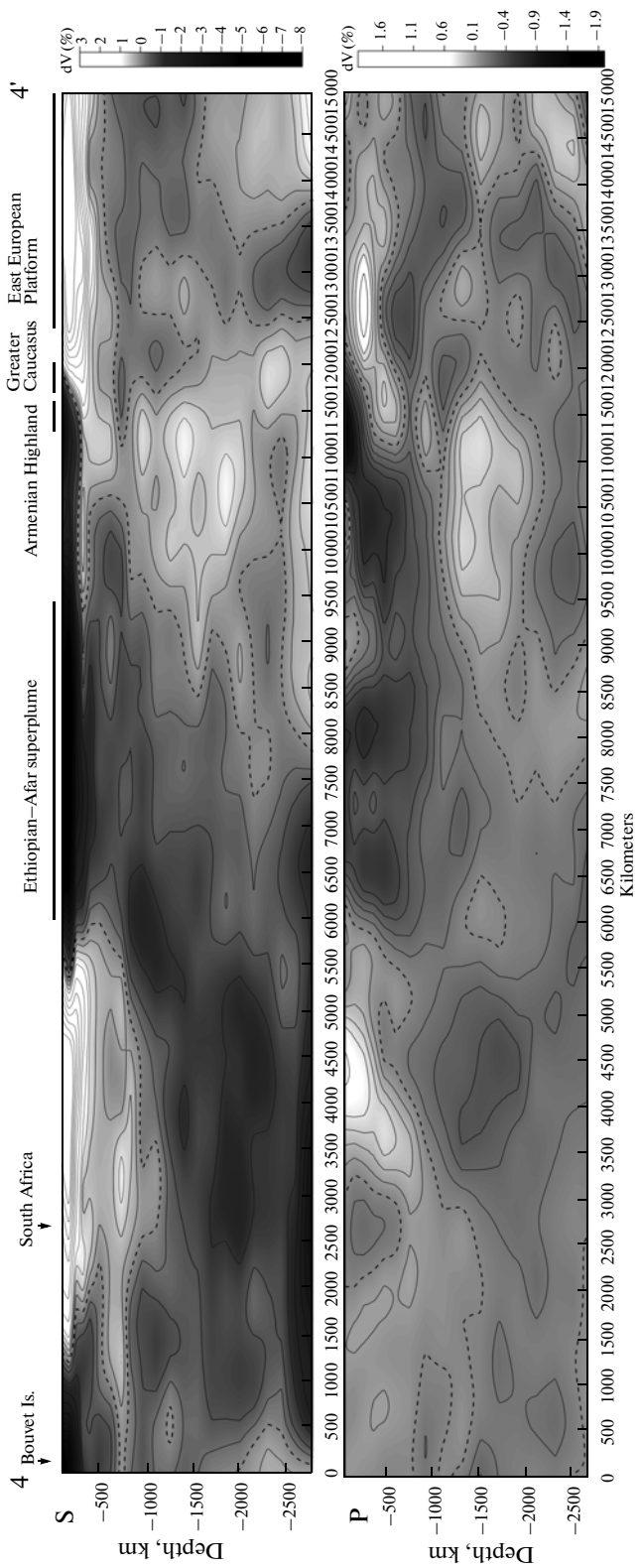

Fig. 5. Seismic tomographic dV_s and dV_p sections along line 4–4' from Bouvet Island via the African Platform, Ethiopian–Afar superplume, Arabian Plate, and the Caucasus to the East European Platform. Compiled by S.Yu. Sokolov after the data published in [43, 47, 60]. Contour lines are spaced at 0.5% for S-waves and 0.25% for P-waves; the dashed line corresponds to zero value.

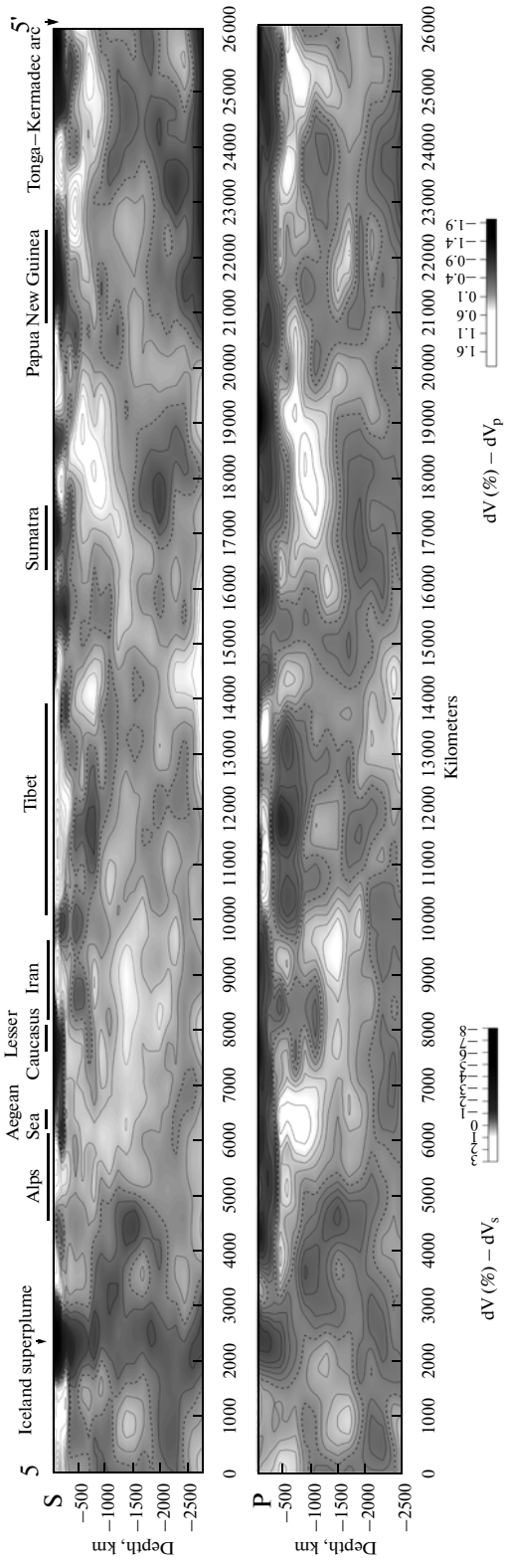

Fig. 6. Seismic tomographic dV_s and dV_p sections along line 5–5' along the Alpine–Himalayan Belt from the Tonga–Kermadec arc via the Indonesian backarc basin, Tibet, Pamir, the Lesser Caucasus, Anatolia, the Carpathians, West European Hercynides to Iceland. Compiled by S.Yu. Sokolov after the data published in [43, 47, 60]. Contour lines are spaced at 0.5% for S-waves and 0.25% for P-waves; the dashed line corresponds to zero value.

tions in combination with geochemical and petrologic data show that in the south of the Armenian Highland, magmas were generated under a pressure corresponding to the upper mantle, whereas in the Greater Caucasus they are lower crustal in origin [12, 13]. A body of low-velocity rocks with elevated electrical conductivity, which was revealed beneath Mount Elbrus at a depth of 35–50 km, is interpreted as a magma source [14]. At the same time, the Sr, Nd, and O isotopic compositions of the igneous rocks and high $^3He/^4He$ ratio indicate that mantle material was supplied to the sources of the Elbrus and Kazbek volcanoes [4, 8, 25]. The basalts of the Armenian Highland are similar in composition to the basalts of the ensialic island arcs and active continental margins [10]. Taking this circumstance into account, Koronovsky and Demina [13] proposed a model according to which lower crustal and uppermost mantle sources were formed owing to heat and mass transfer and oxidation of reduced fluids from deeper mantle levels. In addition to sublithospheric flow, heat release related to the deformation of slabs of the Mesothetian oceanic crust retained in the lithosphere could have been a source of energy necessary for magma generation. Both sources of energy existed in the Armenian Highland, where volcanic activity was particularly intense.

The lower V_s values beneath the mid-ocean ridges and the adjacent parts of the oceans support the model according to which the lithospheric plates move away from the spreading zones on flows of the upper asthenosphere. At the same time, the lower V_s values are not detected deeper than 300 km beneath most spreading zones. What sustains these flows? The Late Cenozoic volcanism of Arabia and the adjacent segments of the Alpine–Himalayan belt is satisfactorily explained by the impact of lateral sublithospheric flow from the Ethiopian–Afar superplume. It may be suggested that such flows from superplumes at the level of the lower asthenosphere maintained magma formation and spreading in the mid-ocean ridges. It is noteworthy that the direction of the lower flows does not often coincide with the direction of spreading controlled by the upper asthenospheric flows. In other words, within-asthenosphere convection can be assumed. Just as the flow from the Ethiopian–Afar superplume has lost its characteristic geochemical attributes during movement, the flows propagating from superplumes to mid-ocean ridges also did not retain these attributes, which are unknown in shallow-seated MORB magma chambers.

Turning back to the Ethiopian–Afar superplume, it is worth noting that the latter is an extended nearly meridional zone which involves the entire belt of volcanic rifts in East Africa. Before the Cenozoic this zone was probably even longer. When the Tethys ocean arose in the Late Paleozoic, fragments of wandering Gondwana, which turned out to lie above the superplume, underwent rifting that developed into spreading. A flow of heated and enriched asthenospheric

material, moving away from the superplume, accelerated displacement of torn-off fragments of Gondwana toward Eurasia, where the oceanic Tethian lithosphere was subducted and the fragments of Gondwana accreted to Eurasia. Because of this, the subduction zone rolled back. As a result, a series of microplates separated by sutures, accretionary bodies, and magmatic occurrences related to various stages of the Tethian evolution arose on the place of the future Alpine–Himalayan belt. In the seismic tomographic sections across the Ethiopian–Afar superplume and the Arabian–Iranian segment of the orogenic belt, the trails of sublithospheric flow are marked by lower seismic wave velocities throughout the upper mantle; the flow is better expressed in the dV_p section (Fig. 5). The flow trails are also seen in section 3–3' (Fig. 4), where such relics directly underlie the thin lithosphere of the Indian Ocean, but to the north, a lens with elevated dV_p values appears above the flow. The overlying lens corresponds to the thickened lithosphere of the Indian Plate and High Asia. The sheet of slightly lowered dV_p values outlined in the lower mantle is tilted to the southwest as the Ethiopian–Afar superplume. This sheet probably is a relic of a previously existing plume.

Counterparts of the structural elements delineated in the northeastern framework of the Pacific Ocean (high-velocity bodies of subduction zones passing into large mantle wedges (LMW) in the lower mantle [7]) are also known in the southeastern Indonesian segment of the belt, but disappear in the Pamir–Himalayan (Tibet) segment, where a bulge of the upper high-velocity layer beneath Southern Tibet (down to 400 km in the dV_s section) and a lens with slightly elevated V_s at a depth of ~600 km may be the LMW relics. In the dV_p section, these lenses are separated by a low-velocity layer, which continues a system of sublithospheric flows related to the Ethiopian–Afar superplume.

The difference between the segments is related to their distinct Cenozoic history. If the island-arc structure of the Indonesian segment has remained until now, then in the Pamir–Himalayan segment, the last relics of the Neotethys were closed in the Oligocene. The relics of the Neotethys and the related backarc basins in the Arabian–Iranian segments were closed from the late Eocene to the middle Miocene. In line with this, subduction and related mantle wedges gave way to collision of the Eurasian and Gondwanan lithospheric plates. Their convergence was slowed down, but a hot asthenospheric flow from the Ethiopian–Afar superplume probably prolonged its movement and gradually spread under the entire orogenic belt. This event developed asynchronously. For example, the sublithospheric low-velocity layer sharply thinned beneath the Greater Caucasus. This thinning could have been caused by thrusting of the Paratethian Caucasus troughs under the Lesser Caucasus before the middle Miocene [15], and subduction hindered the northward propagation of the sublithospheric flow.

The hot lithospheric flow reworked the upper mantle of the Alpine–Himalayan belt. This is expressed in the reduced average V_p in the upper mantle beneath all mountain systems except a part of the Himalayan–Tibetan region (Figs. 2, 6). The decrease in the average velocities can be interpreted as thinning of the lithosphere and the lower crust at the expense of the asthenosphere and/or or as decrease in the density of the lithospheric mantle and the lower crust under the effect of the asthenosphere. Beneath High Asia, where the lithosphere was thickened by Cenozoic deformations, a high-velocity layer up to 300 km thick remained above the low-V_p layer. On moving, the sublithospheric flow enriched in aqueous fluids derived from the mantle wedges related to subduction zones. The asthenosphere activated in this manner or the fluid penetrating into the lithosphere gave rise to a number of Cenozoic geological processes, the consideration of which is out of the scope of this paper. These processes are only denoted below.

The effect of the active asthenosphere and related fluids provoked the formation of within-lithosphere magmatic sources, including crustal ones [19], and induced softening of the lithosphere [3]. This resulted in intense deformations, tectonic delamination, and large lateral displacements. In the presence of fluids, phase transformation of minerals accelerated, in particular in the lower crustal metabasic rocks and in the relics of oceanic crust slabs retained in the lithosphere. This, in turn, changed the density and wave velocities and, as a result, the localization of the Moho discontinuity. Beneath the mountain systems, the destroyed lithospheric mantle was partly replaced with low-density asthenospheric material. In addition to the decompaction of the lower crustal rocks under the effect of asthenospheric fluids, this factor was the main cause of rapid mountain building in the Pliocene and Quaternary. The aforementioned processes reflected in the seismic tomographic data are substantiated by geological and geophysical data obtained for particular mountain systems of the belt [2, 3, 35, 36].

CONCLUSIONS

The consideration of seismic tomographic data on the Ethiopian–Afar superplume and the Alpine–Himalayan Orogenic Belt has shown that lateral flows of the upper mantle material played the crucial role in the Cenozoic tectonic evolution. As follows from the performed analysis and the correlation of its results with geological data, two groups of mantle processes have interacted since the Late Paleozoic and the contribution of each group has changed with time.

First, the Ethiopian–Afar superplume as a meridional body of hot, low-velocity matter ascending from the bottom of the lower mantle operated continuously. Currently its sublithospheric segment occurs beneath the volcanic rifts of the Red Sea and East Africa. It cannot be ruled out that in the Mesozoic the super-

plume propagated even southward. At the upper-mantle level, the superplume passed in a lateral flow, which was characterized by the lowest seismic wave velocities immediately under the lithosphere. The fragments of the moving Gondwanan plates, wandering above the plume, underwent rifting followed by spreading, and their fragments were transported by the flows in the northeastern direction toward Eurasia. Lithotectonic trails of the Paleo-, Meso-, and Neotethys mark the stages of this process. Second, the mantle structural elements of another type—subducted cold slabs, partly or completely passing in the mantle wedges (near-horizontal lenses with increased V_p and V_s) at a depth of 400–800 km—were formed at the active margins of Eurasia, often developing as island arcs.

At present, the second type of the processes is retained in the Indonesian segment of the Alpine–Himalayan Belt. In its northwestern part, the relics of Tethys and its backarc basins were closed from the Eocene to middle Miocene. Collision hindered convergence of the Gondwanan lithospheric plates with Eurasia but did not influence hot asthenospheric flow. As the basins were being closed, this flow destroyed subducted slabs and mantle wedges as their extension and propagated up to the northern margins of the orogenic belt, having reworked the previous structure of the upper mantle. Now, the asthenospheric flow reaches the Greater Caucasus, propagating into the Indian Ocean and extending further beneath the cold continental lithosphere of the Indian Plate and High Asia with increased V_p and V_s. In the Arabian–Caucasus segment of the belt, the stages of this flow are marked by abrupt rejuvenation of collision volcanism in the northern direction and by thinning of the flow beneath the Greater Caucasus, where it has penetrated in the last turn. In the Tibetan segment, the thickening of the cold lithosphere beneath High Asia and the lens with slightly increased V_s beneath Southern Tibet may be trails of former slabs and mantle wedges. On moving, the hot flow became enriched in aqueous fluids derived from the reworked slabs and mantle wedges. The impact of such active asthenosphere on the lithosphere led to the intense Late Cenozoic deformation and was the main factor of mountain building in the Pliocene and Quaternary.

ACKNOWLEDGMENTS

This study was supported by the Division of the Earth Sciences, Russian Academy of Sciences (programs nos. 6 and 9), the Presidium of the RAS (program no. 4), and the Russian Foundation for Basic Research (project no. 11-05-00628-a).

REFERENCES

1. D. L. Anderson and A. M. Dziewonski, "Seismic Tomography," Sci. Amer. **251** (4), 60–68 (1984).
2. E. V. Artyushkov, *Physical Tectonics* (Nauka, Moscow, 1993) [in Russian].
3. E. V. Artyushkov, "Abrupt Continental Lithosphere Weakening as a Precondition for Fast and Large-Scale Tectonic Movements," Geotectonics **37** (2), 107–123 (2003).
4. S. N. Bubnov, Yu. V. Goltsman, and B. G. Pokrovsky, "Sr, Nd, and O Isotopic Systems As Indicators of Origin and Evolution of Primary Melts of Recent Lavas in the Elbrus Volcanic Region, the Greater Caucasus," in *Proceedings of 14th Symposium on Isotope Geochemistry* (GEOKhI, Moscow, 1995), pp. 28–29 [in Russian].
5. N. L. Dobretsov, A. G. Kirdyashkin, and A. A. Kirdyashkin, *Deep Geodynamiocs* (GEO, Novosibirsk, 2001) [in Russian].
6. A. V. Ershov and A. M. Nikishin, "Recent Geodynamics of the Caucasus–Arabia–East Africa," Geotectonics **38** (2), 123–136 (2004).
7. D. Zhao, F. Piraino, and L. Liu, "Structure and Dynamics of the Mantle beneath Eastern Russia and Adjacent Regions," Geol. Geofiz. **51** (9), 1188–1203 (2010).
8. D. A. Ivanov, S. N. Bubnov, V. M. Volkova, et al., "Sr and Nd Isotopic Composition of Quaternary Lavas in the Greater Caucasus in Connection with Their Petrogenesis," Geokhimiya **31** (3), 343–353 (1993).
9. N. A. Imamverdiev, *Geochemistry of the Late Cenozoic Volcanic Complexes of the Lesser Cucasus* (Nafta-Press, Baku, 2000) [in Russian].
10. Yu. V. Karyakin, *Geodynamics of Formation of Volcanic Complexes of the Lesser Caucasus* (Nauka, Moscow, 1989) [in Russian].
11. V. I. Kovalenko, V. V. Yarmolyuk, and O. A. Bogatikov, "Geodynamic Setting of Recent Volcanism in North Eurasia," Geotectonics **43** (5), 337–357 (2009).
12. N. V. Koronovsky and L. I. Demina, "Collision Stage of the Evolution of the Caucasus Sector of the Alpine Foldbelt: Geodynamics and Magmatism," Geotectonics **33** (2), 102–118 (1999).
13. N. V. Koronovsky and L. I. Demina, "Late Cenozoic Volcanism of the Greater Caucasus," in *The Greater Caucasus in the Alpine Epoch* (GEOS, Moscow, 2007), pp. 251–284 [in Russian].
14. *Recent and Contemporary Volcanism of Russia*, Ed. by N. P. Laverov (Nauka, Moscow, 2005) [in Russian].
15. *The Greater Caucasus in the Alpine Epoch*, Ed. by Yu. G. Leonov (GEOS, Moscow, 2007) [in Russian].
16. F. A. Letnikov, "Maturity of Lithospheric Blocks and Endogenic Mineralization," in *Deep Conditions of Endogenic Ore Formation* (Nauka, Moscow, 1986), pp. 16–24 [in Russian].
17. F. A. Letnikov, *Petrology and Fluid Regime of the Continental Lithosphere* (Nauka, Novosibirsk, 1988) [in Russian].
18. F. A. Letnikov, "Ultradeep Fluid Systems of the Earth and Problems of Ore Formation," Geol. Ore Deposits **43** (4), 259–273 (2001).
19. F. A. Letnikov, "Magma-Forming Fluid Systems of the Continental Liothosphere," Geol. Geofiz. **44** (12), 1262–1269 (2003).

20. F. A. Letnikov, "The Nature of Deep-Seated Granite-Forming Fluid Systems," Dokl. Earth Sci. **391** (5), 760–762 (2003).
21. F. A. Letnikov, "Fluid Regime of Endogenic Processes and Ore Formation," Geol. Geofiz. **47** (12), 1296–1307 (2006).
22. L. I. Lobkovsky and V. D. Kotelkin, "Oceanic History and Asymmetry of the Earth from the Viewpoint of Thermochemical Mantle Convection," in *Tectonics and Geodynamics of Phanerozoic Foldbelts and Platforms* (GEOS, Moscow, 2010), Vol. 1, pp. 423–427 [in Russian].
23. A. S. Monin, *Hydrodynamics of Atmosphere, Ocean and Earth's Subsurface* (Gidrometeoizdat, St. Petersburg, 1999) [in Russian].
24. E. Otani and D. Zhao, "Water in Deep Processes in the Upper Mantle and Transitional Layer: Dehydration of Stagnant Subduction Plates and Its Implication for the Large Mantle Wedge," Geol. Geofiz. **50** (12), 1375–1392 (2009).
25. B. G. Polyak, I. L. Kamensky, E. M. Prasolov, et al., "Helium Isotopes in Gases of the Northern Caucasus: Implications for Heat and Mass Influx from the Mantle," Geochem. Int. **36** (4), 329–342 (1998).
26. V. A. Pugin and N. I. Khitarov, *Experimental Petrology and Deep Magmatism* (Nauka, Moscow, 1978) [in Russian].
27. Yu. M. Pushcharovsky, "Three Paradigms of Geology," Geotektonika **29** (1), 4–11 (1995).
28. Yu. M. Pushcharovsky and D. Yu. Pushcharovsky, *Geology of the Earth's Mantle* (GEOS, Moscow, 2010) [in Russian].
29. A. E. Ringwood, *Composition and Petrology of the Earth's Mantle* (McGraw–Hill, New York, 1975; Nedra, Moscow, 1981).
30. I. D. Ryabchikov, "Mantle Magmas as a Sensor of the Composition of Deep Geospheres," Geol. Ore Deposits **47** (6), 455–468 (2005).
31. S. A. Silant'ev and S. Yu. Sokolov, "Effect of Rheological Heterogeneity of the Mantle beneath Axial Zone of Mid-Atlantic Ridge on Isotopic Geochemical Parameters of Magmatism and Distribution of Hydrothermal Ore Occurrences," in *Proceedings of Sci. Conference on New Perspective in Study of Magma and Ore Formation* (IGEM RAN, Moscow, 2010), pp. 153–154 [in Russian].
32. S. Yu. Sokolov, "Structure of the Mantle from Tomographic Data: Transantlatic Near-Latitudinal Section across MAR at the Latitude of the Kane Fracture Zone," in *Proceedings of the 43rd Tectonic Conference on Tectonics and Geodynamics of Phanerozoic Foldbelts* (GEOS, Moscow, 2010), Vol. 2, pp. 293–296 [in Russian].
33. O. G. Sorokhtin, *Life of the Earth* (Regular and Chaotic Dynamics Sci.-Inform. Center, Moscow–Izhevsk) [in Russian].
34. O. G. Sorokhtin and S. A. Ushakov, *Evolution of the Earth* (Moscow State Univ., Moscow, 2002) [in Russian].
35. V. G. Trifonov, "Age and Mechanism of Recent Mountain Building," in *Proceedings of the 41st Tectonic Conference* (GEOS, Moscow, 2008), Vol. 2, pp. 349–353 [in Russian].
36. V. G. Trifonov, E. V. Artyushkov, A. E. Dodonov, D. M. Bachmanov, A. V. Mikolaichuk, F. A. Vishnyakov, "Pliocene–Quaternary Mountain Building in the Central Tien Shan," Geol. Geofiz. **49** (2), 128–145 (2008).
37. V. G. Trifonov, O. V. Soboleva, R. V. Trifonov, and G. A. Vostrikov, *Contemporary Geodynamics of the Alpine–Himalayan Collision Belt* (GEOS, Moscow, 2002) [in Russian].
38. V. P. Trubitsin, "The Tectonics of Floating Continents," Herald Russ. Acad. Sci. **75** (1), 7–18 (2005).
39. S. A. Fedotov, "Deep Structure, Properties of the Upper Mantle and Volcanic Activity of the Kurile–Kamchatka Island Arc from Seismological Data as of 1964," in *Volcanism and Deep Structure of the Earth* (Nauka, Moscow, 1966), pp. 8–25 [in Russian].
40. V. V. Yarmolyuk, O. A. Bogatikov, and V. I. Kovalenko, "Late Cenozoic Transcontinental Structures and Magmatism of the Earth's Euro-African Segment and Geodynamics of Its Formation," Dokl. Earth Sci. **395** (2), 183–186 (2004).
41. R. Altherr, F. Henjes-Kunst, and A. Baumann, "Asthenosphere Versus Lithosphere as Possible Sources for Basaltic Magmas Erupted during Formation of the Red Sea: Constraints from Sr, Pb and Nd Isotopes," Earth Planet. Sci. Lett. **96**, 269–286 (1990).
42. D. L. Anderson, "Speculations on the Nature and Cause of Mantle Heterogeneity," Tectonophysics **416**, 7–22 (2006).
43. J. A. Baker, M. A. Mensies, M. F. Thirlwall, and C. G. MacPherson, "Petrogenesis of Quaternary Intraplate Volcanism, Sana'a, Yemen: Implications for Plume–Lithosphere Interaction and Polybaric Melt Hybridization," J. Petrol. **36**, 1359–1390 (1997).
44. T. W. Becker and L. Boschi, "A Comparison of Tomographic and Geodynamics Mantel Models," G-Cubed Geochem. Geophys. Geosystems **3**, 2002, 2001GC000168, http://www.geophysics.harvard.edu/geodyn/tomography/
45. H. Bertrand, G. Chazot, J. Blichert-Toft, and S. Thoral, "Implications of Widespread High-Volcanism on the Arabian Plate for Afar Mantle Plume and Lithosphere Composition," Chem. Geol. **198**, 47–61 (2003).
46. V. E. Camp and M. J. Roobol, "Upwelling Asthenosphere Beneath Western Arabia and Its Regional Implication," J. Geophys. Res. **97**, 15255–15271 (1992).
47. K. C. Creager and T. H. Jordan, "Slab Penetration into the Lower Mantle," J. Geophys. Res. **89** (B5), 3031–3049 (1984).
48. S. P. Grand, R. D. van der Hilst, and S. Widiyantoro, "Global Seismic Tomography: A Snapshot of Convection in the Earth," GSA Today **7**, 1–7 (1997).
49. J. Huang and D. Zhao, "High-Resolution Mantle Tomography of China and Surrounding Regions," J. Geophys. Res. **111** (B09305), 1–21 (2006).
50. S. D. Jacobsen, S. Demouchy, J. D. Frost, T. B. Ballaran, J. Kung, "A Systematic Study of OH in Hydrous Wadsleyite from Polarized FTIR Spectroscopy and Single-Crystal X-Ray Diffraction: Oxygen Sites for

Hydrogen Storage in Earth's Interior," Am. Mineral. **90** (1), 67–70 (2005).

51. A. Kelbert, A. Schultz, and G. Egbert, "Global Electromagnetic Induction Constraints on Transition-Zone Water Content Variations," Nature **469**, 1003–1006 (2009).
52. J. F. Lawrence and M. E. Wysession, "Seismic Evidence for Subduction-Transported Water in the Lower Mantle," in *Earth Deepwater Cycle*, Ed. by S. V. Jacobsen and S. van der Lee (Geophys. Monograph Series, 2006), Vol. 168, pp. 251–261.
53. M. Lustrino and E. Sharkov, "Neogene Volcanic Activity of Western Syria and Its Relationship with Arabian Plate Kinematics," J. Geodynamics **42**, 115–139 (2006).
54. S. Y. O'Reilly and W. L. Griffin, "Imaging Global Chemical and Thermal Heterogeneity in the Subcontinental Lithospheric Mantle with Garnet and Xenoliths: Geophysical Implications," Tectonophysics **416**, 289–309 (2006).
55. A. Robertson, Ü. C. Unlügenç, N. Inan, and K. Taśli, "The Misis-Andirin Complex: A Mid-Tertiary Melange Related to Late-Stage Subduction of the Southern Neotethys in S. Turkey," J. Asian Earth Sci. **22** (5), 413–453 (2004).
56. A. Segev, "Magmatic Rocks," in *Geological Framework of the Levant*, Ed. by V. A. Krasheninnikov et al. (Historical Production-Hall, Jerusalem, 2005), Vol. 2, Pt. 4, pp. 553–576.
57. J. R. Smyth, "A Crystallographic Model for Hydrous Wadsleyite: An Ocean in the Earth's Interior?," Am. Mineral. **79**, 1021–1025 (1994).
58. M. Stein and A. W. Hofmann, "Fossil Plume Head beneath the Arabian Lithosphere," Earth Planet. Sci. Lett. **114**, 193–209 (1992).
59. H. Thybo, "The Heterogeneous Upper Mantle Low Velocity Zone," Tectonophysics **416**, 53–79 (2006).
60. V. G. Trifonov, A. E. Dodonov, E. V. Sharkov, D. I. Golovin, I. V. Chernyshev, V. A. Lebedev, T. P. Ivanova, D. M. Bachmanov, M. Rukieh, O. Ammar, H. Minini, A.-M. Al Kafri, and O. Ali, "New Data on the Late Cenozoic Basaltic Volcanism in Syria, Applied to Its Origin," J. Volcanol. Geotherm. Res. **199**, 177–192 (2011).
61. R. D. van der Hilst, S. Widiyantoro, and E. R. Engdahl, "Evidence of Deep Mantle Circulation from Global Tomography," Nature **386**, 578–584 (1997).

Reviewers: E.A. Rogozhin and V.V. Yarmolyuk